High Performance Flip-Structure Enhancement-Mode HEMT with Face-to-Face Double Gates

Siyu Deng, Jie Wei, Cheng Zhang, Dezun Liao, Tao Sun, Kemeng Yang, Lufan Xi, Bo Zhang and Xiaorong Luo*

Abstract

A novel double gates flip-structure enhancement-mode (E-mode) high electron mobility transistor with step field plate (DFF HEMT) is proposed. It features face-to-face double gates, including a top trench MIS gate with a step field plate and a bottom planar MIS gate, which is shorted together. In the on-state, the double gates not only can restore the 2DEG by the higher electric potential, but also can form the electron accumulation layers, and thus increase the saturation output current and reduce the on-resistance. The face-to-face double gates together deplete the 2DEG by using the work function difference to realize E-mode, instead of by etching the AlGaN layer under the gate for the conventional MIS gate E-mode HEMT. The double-gate structure not only avoids etch damage, but also maintains both high threshold voltage and low on-resistance. Meanwhile, the step gate field plate modulates *E*-field distribution to increase the *BV*. In order to easily fabricate, the trench gate with step field plate must be located on the top of device, forming the flip-structure. The flip-structure is also beneficial to decrease the leakage current in the substrate. The simulated V_{th}, *BV* and I_d of the DFF HEMT are 0.8 V, 465 V and 494 mA/mm, respectively. The *FOM* of the DFF HEMT is 79.8% and 444.2% higher than those of the conventional MIS-FP HEMT and MIS HEMT.

Keywords: AlGaN/GaN HEMT, Enhancement-mode, Double gates, Flip-structure, Breakdown voltage

Introduction

GaN-based high electron mobility transistor (HEMT) has great prospects in low loss and high power application [1–4], owing to its high density two-dimensional electron gas (2DEG) and high electron mobility. The conventional GaN HEMT is always depletion mode (D-mode), while the enhancement mode (E-mode) is necessary in power electronics applications. Many structures have been proposed to achieve the E-mode, such as a thinned AlGaN barrier layer [5], p-gate structure [6], recessed gate structure [7], and fluoride ion treatment [8, 9]. All technologies above are realized by depleting the 2DEG under the gate, inevitably encountering a tradeoff between a high threshold voltage (V_{th}) and a large saturated output current ($I_{d, sat}$). Meanwhile, the gate Metal-gate Insulator-AlGaN Semiconductor (MIS) generally has been used for the HEMT with recessed gate.

The breakdown voltage (*BV*) of the GaN HEMT is far below its theoretical limit because the E-field crowding causes premature breakdown at the edge of gate. To solve this problem, several technologies have been adopted, including field plate (FP) [10, 11], RESURF technology [12, 13] and polarization junction concept [14, 15]. However, there is also a tradeoff relationship between the high *BV* and $I_{d, sat}$, owning to the assisted depletion on the 2DEG of the drift region.

Recently, a flip-structure has been proposed [16]. By the substrate transferring technology, the device is located on the poly-AlN, which reduces the leakage of Si substrate. Importantly, the flip-structure facilitates

*Correspondence: xrluo@uestc.edu.cn

The State Key Laboratory of Electronic Thin Films and Integrated Devices, University of Electronic Science and Technology of China, Chengdu 610054, China

Deng *et al. Nanoscale Research Letters*   (2022) 17:73

Page 2 of 9

the monolithic integration of the HEMT and the vertical LED.

In this paper, a novel double gates flip-structure enhancement-mode (E-mode) HEMT with field plate (DFF-HEMT) is proposed. Its on-state and off-state electrical characteristics are studied by simulation. The simulated results show that DFF-HEMT can significantly improve the on-state, off-state characteristics and realize E-mode.
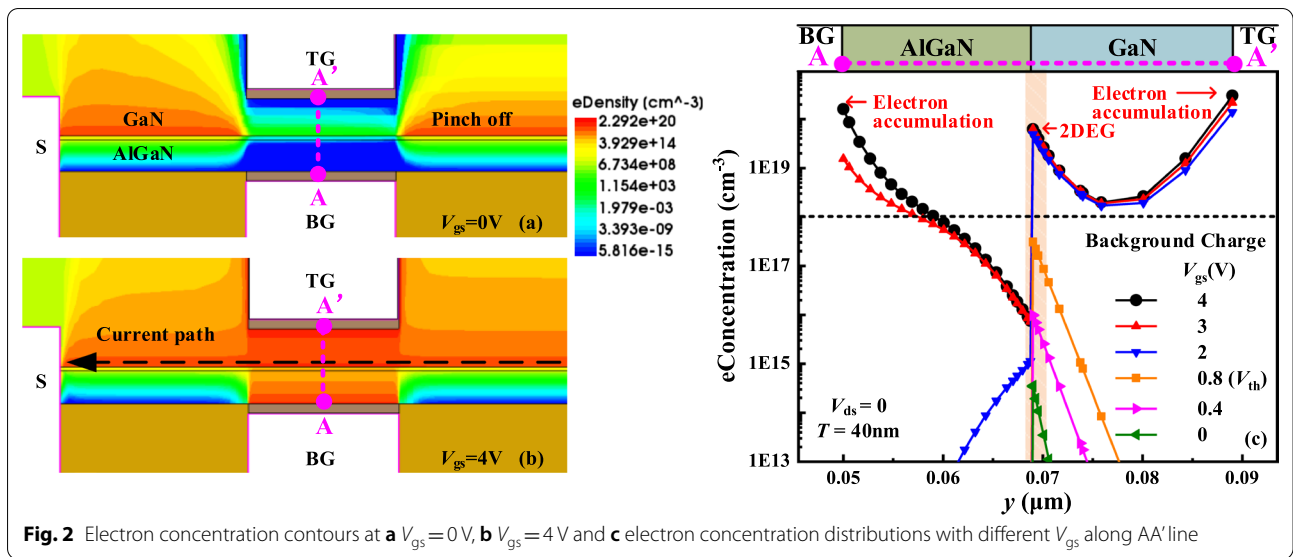
Device Structure and Mechanism

Figure 1a and b are the schematic section of the proposed DFF HEMT. The DFF HEMT has the following two features. One is the face-to-face double gates, including a top trench MIS gate with step field plate (TG) and a bottom planar MIS gate (BG), and they are shorted together, as shown in Fig. 1a. In order to easily fabricate, the trench gate with step field plate must be located on the top of device. So, the other feature is a flip-structure, of which the source, the bottom gate and the drain are below the 2DEG channel instead of above the 2DEG channel. The length of the step field plate is L, and the thickness of the semiconductor between the double gates is T as shown in Fig. 1b, and $T = 40$ nm and $L = 2.6$ μm are fixed except especial statement. The thickness of Al_2O_3 layer is 10 nm and the height of the step field plate is 200 nm. The x- and y-direction are given. The conventional MIS trench gate HEMT (MIS HEMT) and the MIS trench gate HEMT with field plate (MIS-FP HEMT) are shown in Fig. 1c and

d. The thickness of passivation layer, AlGaN barrier layer and GaN buffer layer are 50 nm, 19 nm and 1 μm for three devices, and the lateral dimensions of drift region $L_{gd} = 5$ μm (the distance between the gate and drain) for the two device is the same as that of the DFF HEMT. The length of the field plate is 2.3 μm for the MIS-FP HEMT. The metal work function is 5.15 eV. Several important physical models have also been considered, such as narrowing of the band gap, high field saturation, doping dependency and Shockley–Read–Hall [17]. The mobility of the 2DEG under the gate has been set as 680 cm²/V·s [18] and the electron mobility of the MIS interface has been set as 100 cm²/V·s [19] because of the etch damage.

The gate metal, Al_2O_3 and semiconductor AlGaN or GaN constitute top and bottom two MIS structures. Figure 2 shows the electron concentration contours and distributions along AA' line under the different V_{gs} values. At $V_{gs} = 0$, 2DEG between the double gates is almost depleted by the double gates owing to the work function difference between the gate metal and AlGaN or GaN, as shown in Fig. 2a and c. Therefore, the current path is pinched off and E-mode is realized. The conventional MIS gate realizes the E-mode by etching the AlGaN layer to reduce 2DEG density, which not only introduces etch damage, but also increases the on-resistance and weakens the current capacity. For the DFF HEMT at $V_{gs} > V_{th}$, the 2DEG completely recovers and even form an electron accumulation layer, as shown in Fig. 2b and c. The current path is turned on and effectively increases the
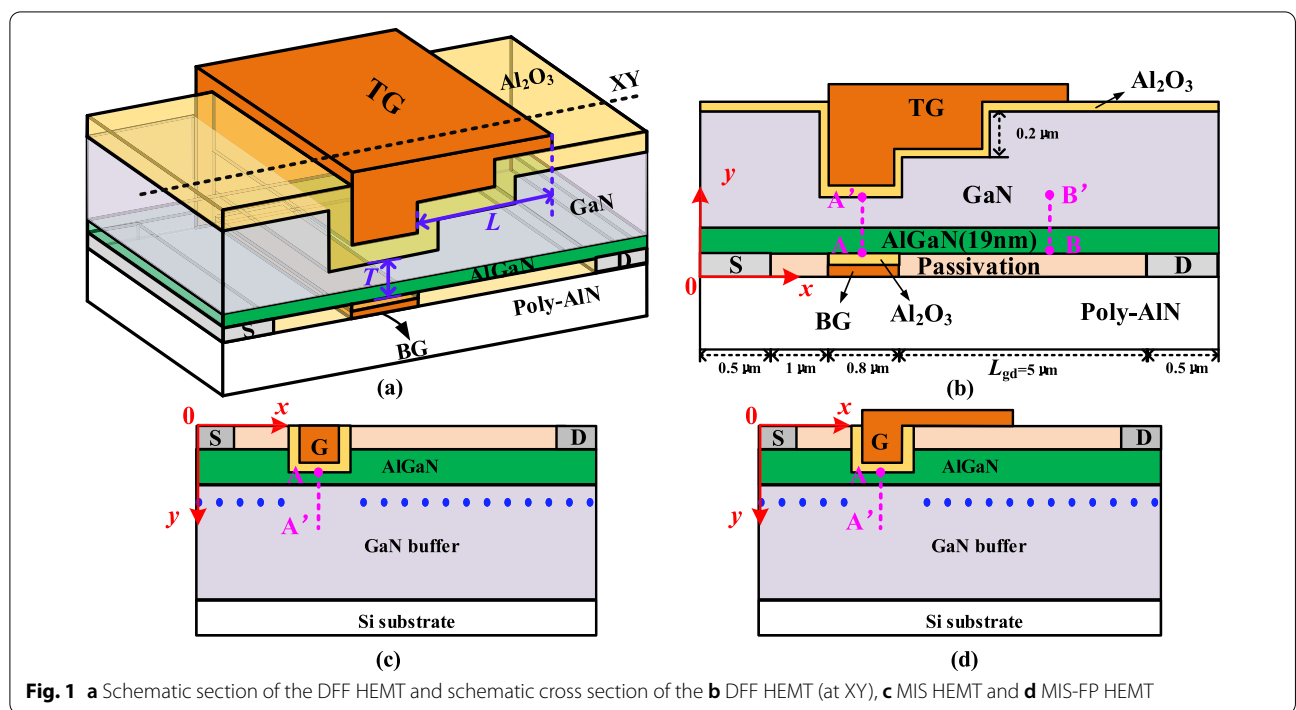
Fig. 1 **a** Schematic section of the DFF HEMT and schematic cross section of the **b** DFF HEMT (at XY), **c** MIS HEMT and **d** MIS-FP HEMT

Fig. 2 Electron concentration contours at **a** $V_{gs} = 0$ V, **b** $V_{gs} = 4$ V and **c** electron concentration distributions with different V_{gs} along AA' line
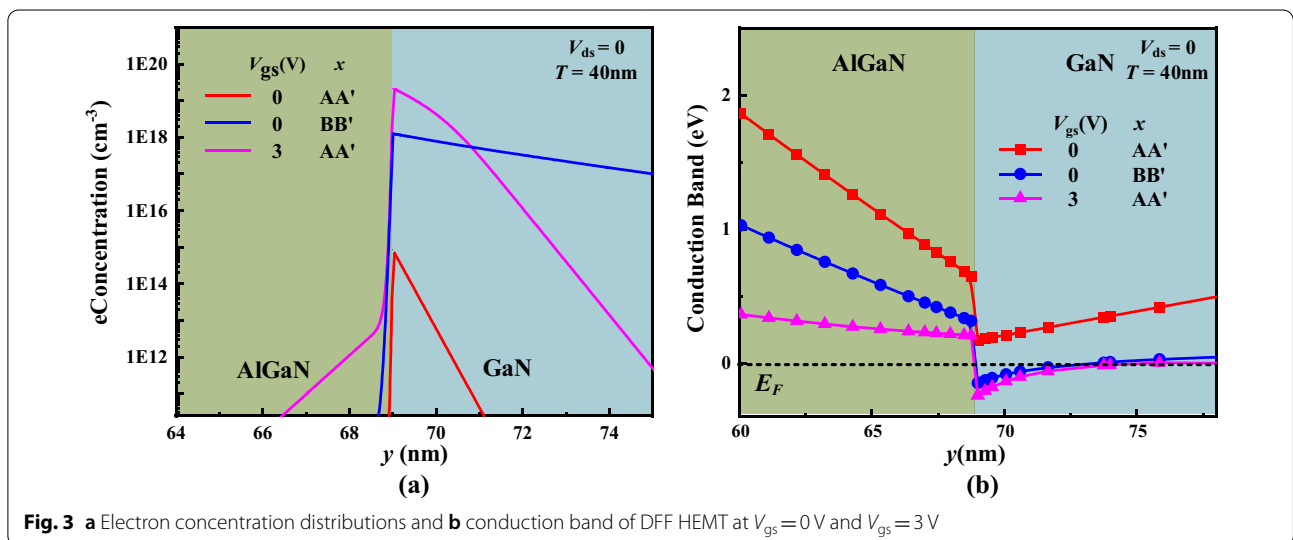
output current. As V_{gs} increases, the 2DEG concentration increases in Fig. 2c. Furthermore, the electron concentration near the sides of two gates is higher than the doping concentration, verifying forming the electron accumulation layer. It breaks through the tradeoff relationship between the high V_{th} and the high output current in GaN HEMT. In the off state, the step field plate effectively improves the *BV* of the DFF HEMT.
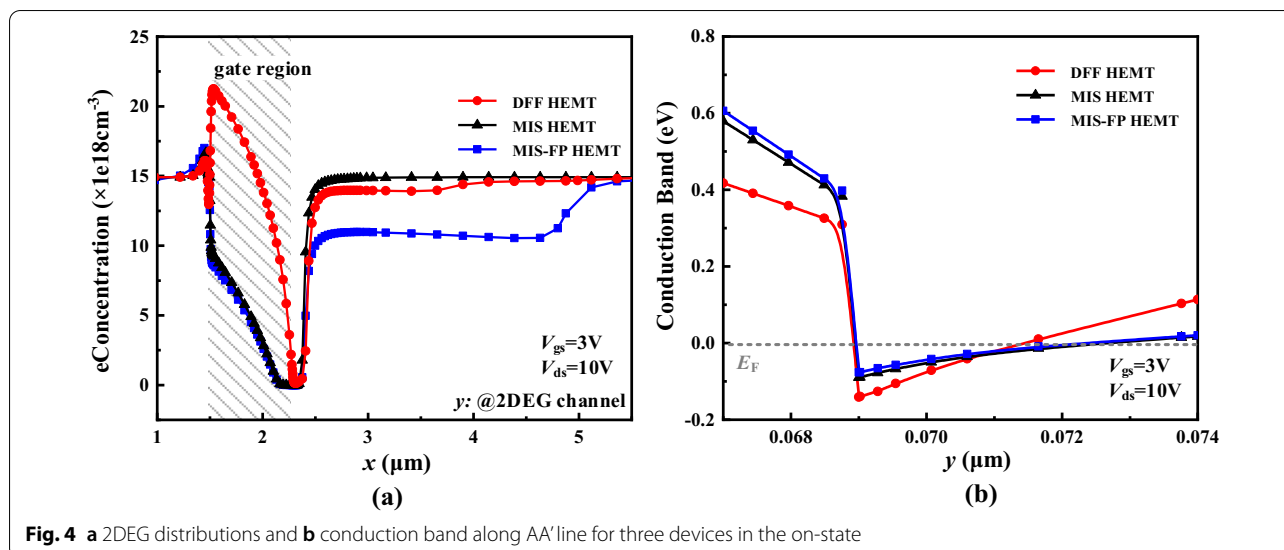
Results and Discussion

Figure 3 shows the electron concentration distributions and conduction band of the DFF HEMT. When $V_{gs} = 0$, the electron density along AA' line (in Fig. 1) is just 5×10^{14} cm^{-3} in Fig. 3a, and the conduction band is

above the Fermi level in Fig. 3b. The E-mode is thus realized. When $V_{gs} = 3$ V $> V_{th}$, the conduction band along AA' line has been pulled below the Fermi level, and electron density is as high as 2×10^{19} cm^{-3}. The DFF HEMT has been turned on. Additional, the electron density along AA' line at $V_{gs} = 3$ V is higher than that along BB' line at $V_{gs} = 0$ V in Fig. 3a. It indicates that 2DEG has been restored owing to high positive-voltage biased to the double gate.

Figure 4a shows the electron concentration distributions along the 2DEG channel in the on-state. The 2DEG concentration of the gate region of the DFF HEMT is much higher than those of the MIS HEMT and the MIS-FP HEMT. On one hand, the potential in the gate region
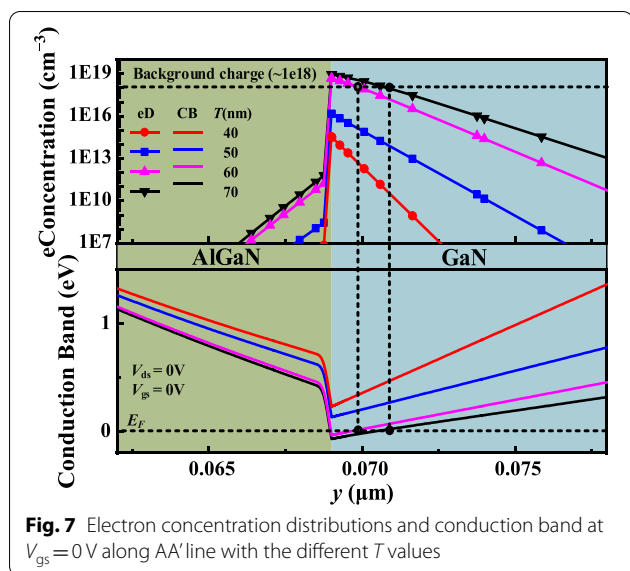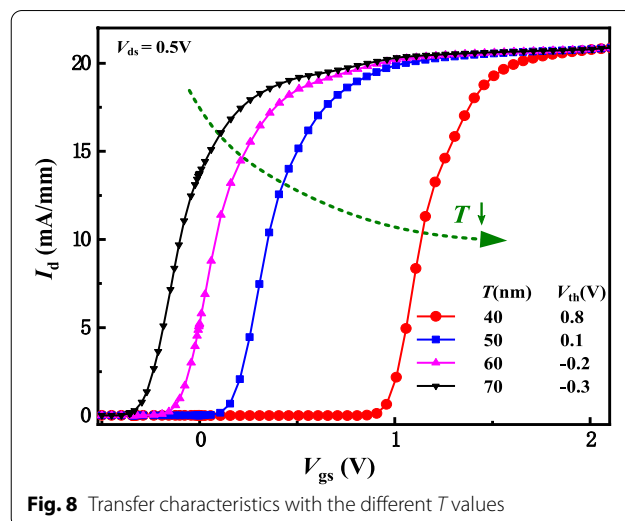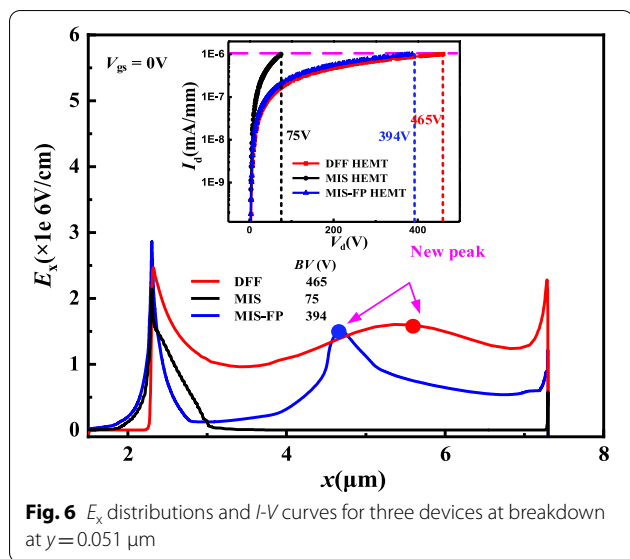

Fig. 3 **a** Electron concentration distributions and **b** conduction band of DFF HEMT at $V_{gs} = 0$ V and $V_{gs} = 3$ V

Deng *et al. Nanoscale Research Letters* (2022) 17:73

Page 4 of 9

Fig. 4 **a** 2DEG distributions and **b** conduction band along AA' line for three devices in the on-state
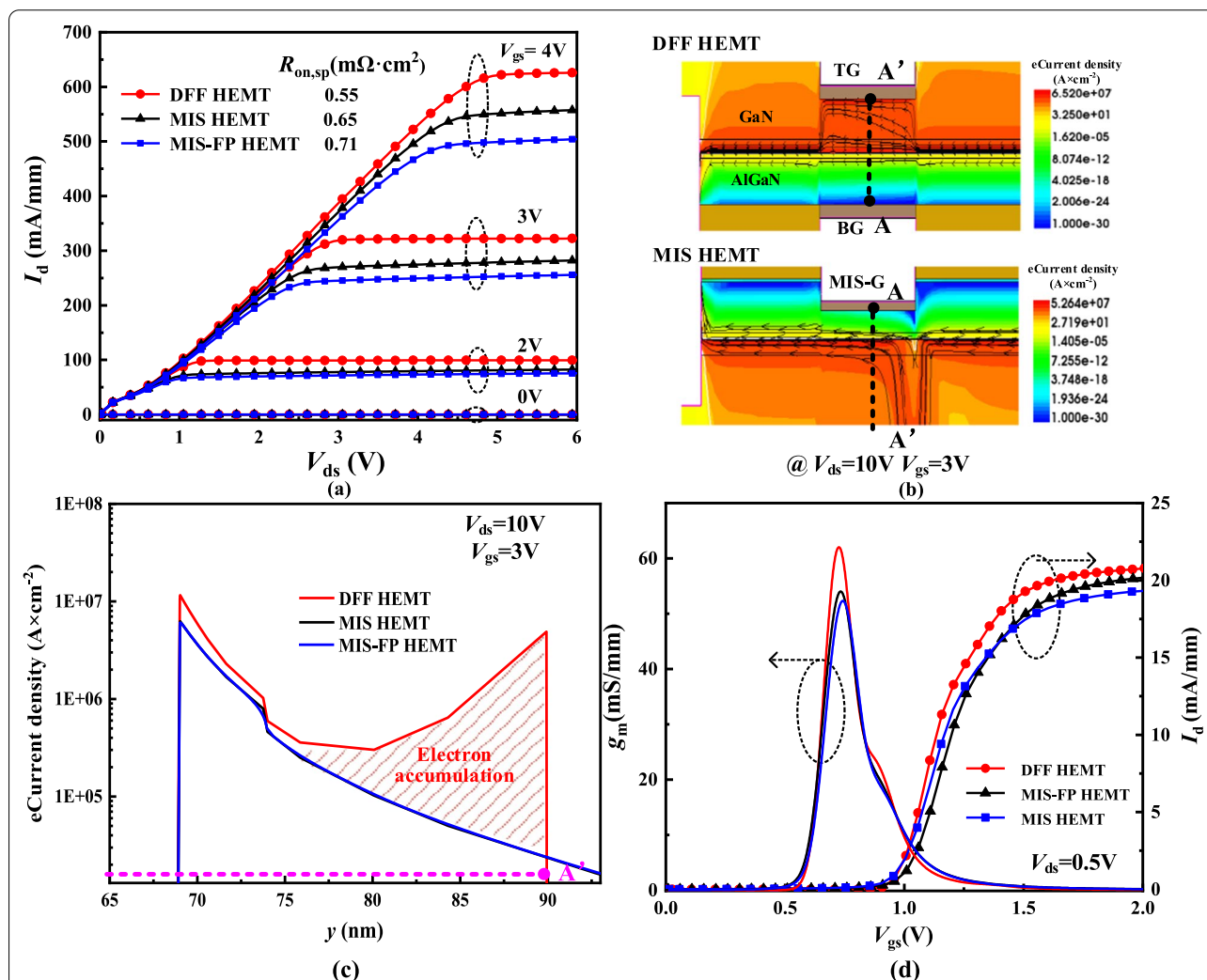
Fig. 5 **a** output *I-V* characteristics, **b** electron current density, **c** electron current density distributions along AA' line and **d** transfer characteristics for three devices

Deng *et al. Nanoscale Research Letters*   (2022) 17:73

Page 5 of 9

Fig. 6 E_x distributions and *I-V* curves for three devices at breakdown at $y = 0.051$ μm

Fig. 8 Transfer characteristics with the different *T* values

Fig. 7 Electron concentration distributions and conduction band at $V_{gs} = 0$ V along AA' line with the different *T* values
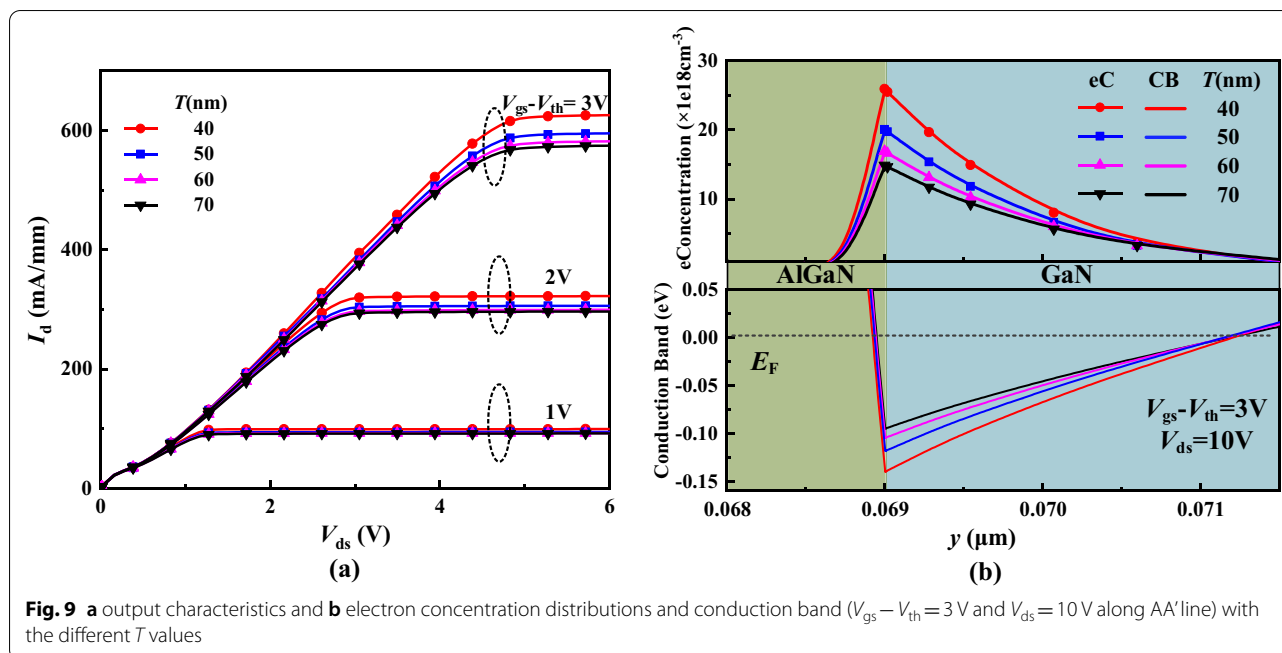
of the DFF HEMT is much higher because both the BG and TG are applied to 3 V. The conduction band of the DFF HEMT is thus much lower as shown in Fig. 4b, which contributes to the higher 2DEG concentration. On the other hand, the polarization effect under the gate of the MIS HEMT and the MIS-FP HEMT is weakened because the AlGaN layer is etched partly to realize E-mode. Additional, it is normal that the 2DEG density under the right side of the gate is low for the three devices, because there is a higher electric potential of the semiconductor than that of the gate, as a depletion region. The field plate of the DFF HEMT is far away from the 2DEG channel and has smaller depletion effect on the 2DEG concentration than that of the MIS-FP HEMT. Therefore, the 2DEG concentration under the field plate of the DFF HEMT is higher, which contributes to higher current and lower specific on-resistance ($R_{on, sp}$).

Figure 5 shows the output characteristic and transfer characteristic of the three devices. It can be seen from Fig. 5a that the DFF HEMT has the largest $I_{d, sat}$ and the smallest $R_{on, sp}$. The $I_{d, sat}$ of the MIS-FP HEMT is the smallest because the field plate assists in depleting 2DEG along the drift region (see Fig. 4a). For the DFF HEMT, on one hand, the 2DEG is recovered, and on the other hand, the double gates introduce electron accumulation layer. Figure 5c shows the electron current density along AA' line. The DFF HEMT has a large current density in electron accumulation layer, in addition to the 2DEG channel current. The 2DEG channel still plays a dominant role in the transport. It can be seen from Fig. 5d that DFF HEMT has the highest transconductance owing to the double gates. The V_{th} of three devices is designed as 0.8 V.

Figure 6 shows the lateral component of the *E*-field (E_x) distribution and *I-V* curves at breakdown. It indicates that the E_x for the DFF HEMT is effectively improved. Compared with the MIS HEMT, the field plate not only brings out new *E*-field peak, but also expands the depletion region for the MIS-FP and DFF HEMT. Particularly, for the DFF HEMT, the step field plate further uniforms the *E*-field distribution in the drift region. Meanwhile, the leakage current of the substrate has been suppressed

Fig. 9 **a** output characteristics and **b** electron concentration distributions and conduction band ($V_{gs} - V_{th} = 3$ V and $V_{ds} = 10$ V along AA'line) with the different T values

by the poly-AlN substrate layer. Therefore, the DFF HEMT achieves the highest BV of 465 V (at $I_d = 10^{-6}$ mA/mm), and BV is 394 V for the MIS-FP HEMT, as shown in Fig. 6. Without the field plate and flip-structure for the MIS HEMT, the drift region cannot be completely depleted and leakage current is large, and thus the BV is just 75 V at the same drift region length.

Figure 7 shows the electron concentration distributions and conduction band at $V_{gs} = 0$ V along AA' line with different T values. As T decreases, the conduction band rises and the electron density decreases. When $T \leq 50$ nm, the depletion effect of the MIS structure on electrons is enhanced and the polarization effect is weakened. The whole conduction band is raised above E_F. Consequently, E-mode is realized. When $T > 50$ nm, the depletion effect is weakened and the polarization effect is enhanced. Therefore, potential well of electrons is formed and the electron concentration rises to 10^{19} cm^{-3} order of magnitude, which is higher than the background charge concentration of 10^{18} cm^{-3}. Figure 8 shows the transfer characteristic with different T values. The V_{th} increases as T decreases.

Figure 9 shows the output characteristic, electron concentration distributions and conduction band with the different T values at a constant of ($V_{gs} - V_{th}$). The $I_{d, sat}$ increases and the $R_{on, sp}$ decrease as T decreases because the electron concentration increases, as shown in Fig. 9a

and b. As T decreases, the V_{th} increases (in Fig. 8) and thus V_{gs} accordingly increases to maintain a constant of ($V_{gs} - V_{th}$), leading to the increase in electron concentration. Meanwhile, the conduction band is lower and the 2DEG concentration is higher owing to the lower T and higher V_{gs}, as indicated in Fig. 9b. Different from the conventional GaN HEMT, the DFF HEMT break through the tradeoff relationship between the high V_{th} and high $I_{d, sat}$. As T decreases, both the $I_{d,sat}$ and the V_{th} increase.

Figure 10 shows the influence of the L on the potential contours and E_x distribution of the DFF HEMT. The BV of the DFF HEMT firstly increases and then decreases as the L increases. When $L = 0$ µm means the DFF HEMT without the field plate, the BV is lower because the drift region has not been depleted. With the increase in L at $L < 2.6$ µm, the depletion region expands. The step field plate decreases the E-field peak at the gate edge (P1) and induces a new E-field peak below the end of the field plate (P2), so the BV increases as shown in Fig. 10b. P3 is the new E-field peak caused by the step field plate at $y = 0.051$ µm in Fig. 10b. At this time, the premature breakdown occurs at the right edge of the gate. When $L = 2.6$ µm, the E_x of the DFF HEMT is almost uniform and the BV of 465 V achieves the highest. When $L = 3.0$ µm, premature breakdown occurs owing to high P2, and BV decreases.

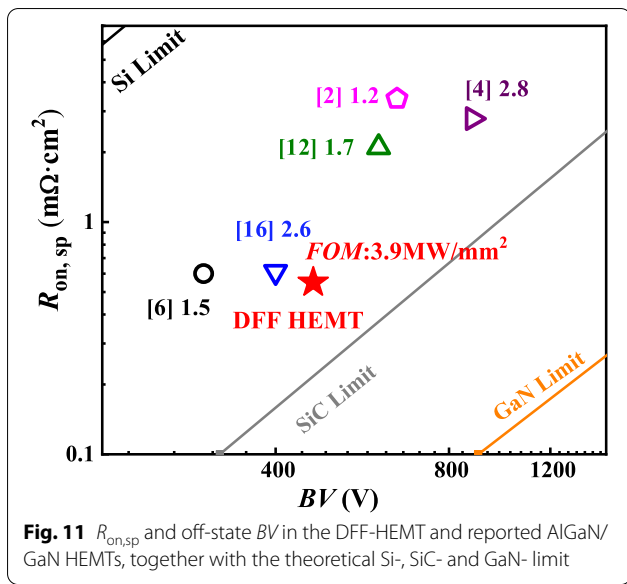Deng *et al. Nanoscale Research Letters*   (2022) 17:73

Page 7 of 9
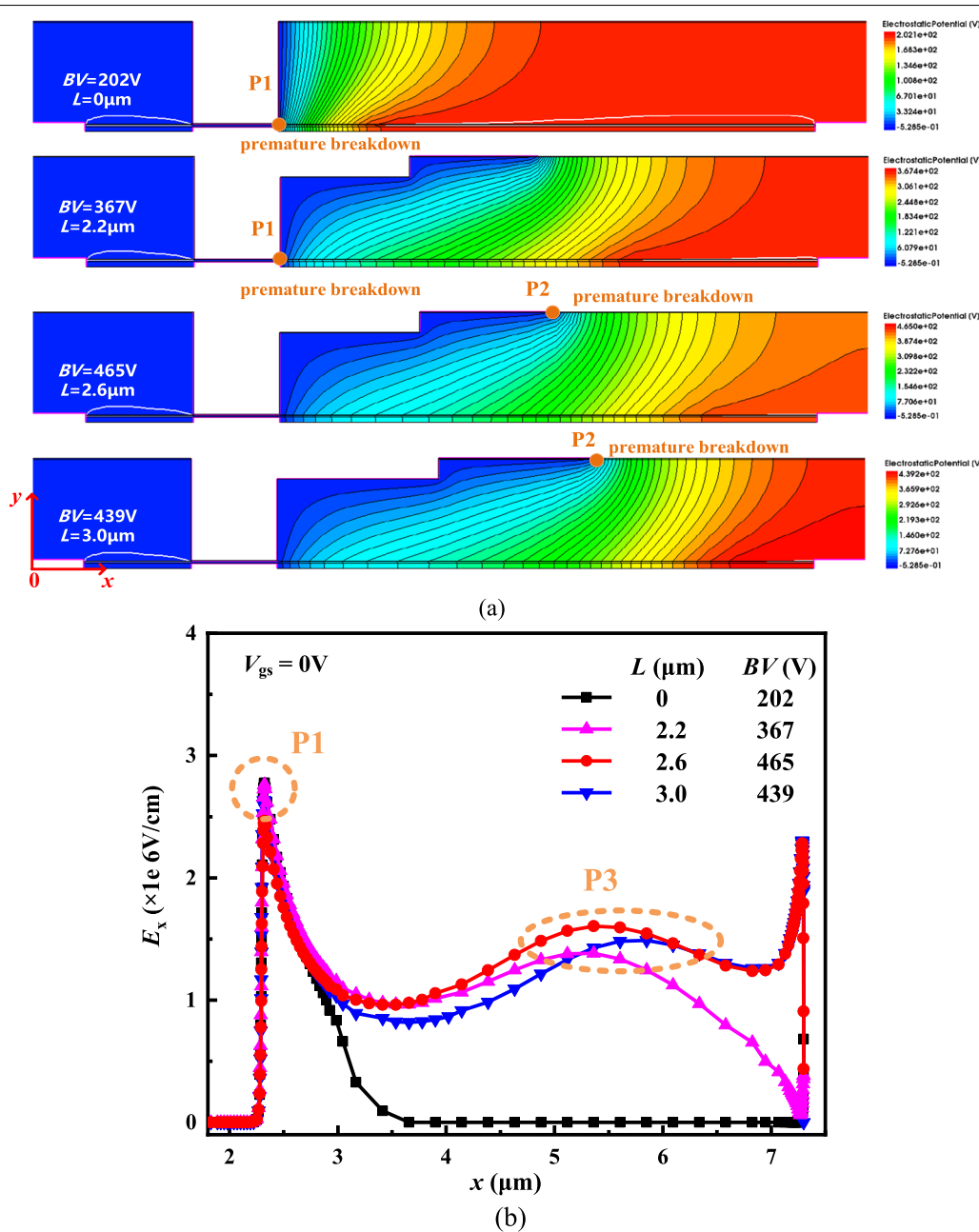
Fig. 10 **a** Equipotential contours and **b** *Ex* distribution at breakdown at $y = 0.051$ μm with different *L* values

Figure 11 demonstrates the $R_{\text{on,sp}}$ and *BV* values of the DFF HEMT and reported AlGaN/GaN HEMTs, the DFF-HEMT has a higher figure of merit (FOM $= BV^2/R_{\text{on,sp}}$) than those of the AlGaN/GaN HEMTs in studies. As a result, when $T = 40$ nm, $L = 2.6$ μm, an excellent tradeoff

between the on-state characteristics and the off-state characteristics is achieved.

The fabrication process steps of the DFF HEMT are shown in Fig. 12, which is referred to the experiment in [16]. Key processes are given as follows: (a) Fabricate a
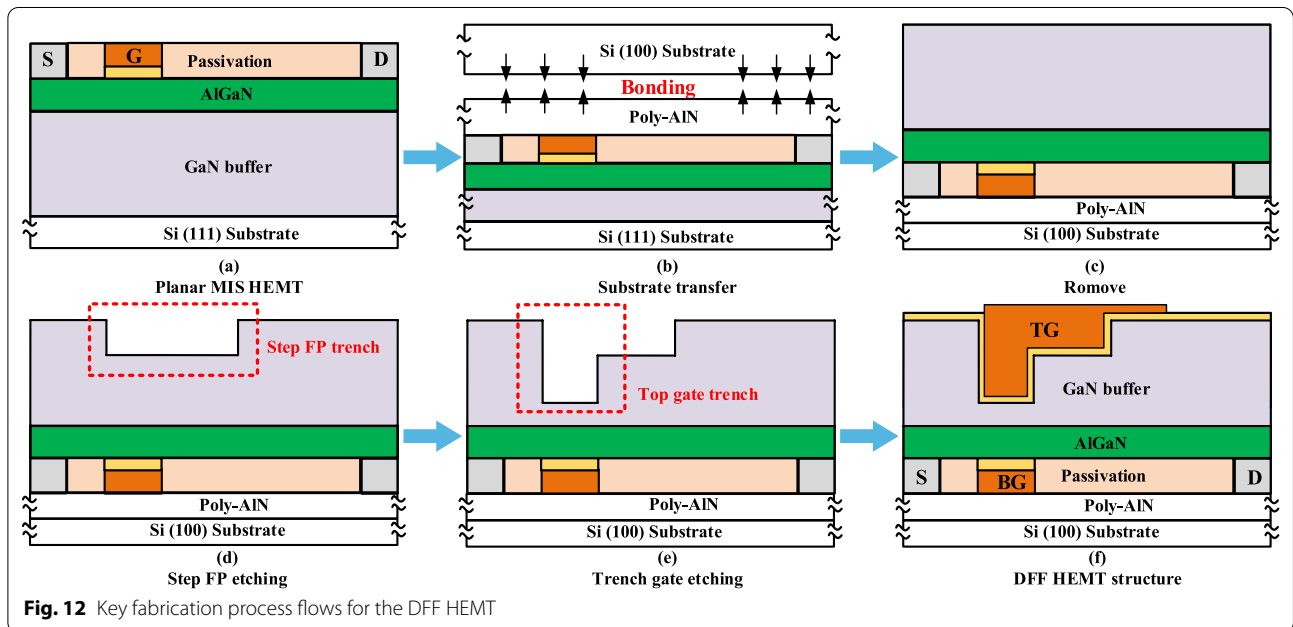
Fig. 11 $R_{on,sp}$ and off-state *BV* in the DFF-HEMT and reported AlGaN/GaN HEMTs, together with the theoretical Si-, SiC- and GaN- limit

conventional MIS HEMT on a Si (111)-based AlGaN/GaN heterojunction wafer. (b) form poly-AlN film on the device surface by physical vapor deposition (PVD), and bonding to the Si (100) wafer. (c) Remove the Si (111) substrate and part of the GaN epitaxial layer. (d) form the shallow trench of the field plate by inductively coupled

plasma (ICP) etching. (e) ICP etch TG deep trench. (f) implement Al_2O_3 layer and the top gate metal. Compared with those of Ref. [16], the fabrication process of the DFF HEMT only add twice ICP etchings ((d) and (e)) to realize the E-mode and further improve the *BV*. The DFF HEMT simultaneously realizes E-mode, and achieves a higher *BV* and a smaller R_{on}.

Conclusion

A novel double-gate flip-device enhancement-mode (E-mode) HEMT is proposed and investigated. It features face-to-face double gates with a top gate with step field plate and a bottom gate. The double gates restore the 2DEG and form the accumulation layers to increase the output current capacity and reduce the on-resistance. The double MIS gates together deplete the 2DEG to realize E-mode by the work function difference. Meanwhile, the step field plate flattens the *E*-field distribution and increase the *BV*. The proposed E-mode GaN power device has many advantages, including E-mode, high voltage and high saturation current capacity. The V_{th}, *BV* and I_d of the DFF HEMT are 0.8 V, 465 V and 494 mA/mm, respectively. The *FOM* of the DFF HEMT is 79.8% and 444.2% higher than that of the conventional MIS-FP HEMT and MIS HEMT.

Fig. 12 Key fabrication process flows for the DFF HEMT

Deng *et al. Nanoscale Research Letters*   (2022) 17:73

Page 9 of 9

Abbreviations
HEMT: High electron mobility transistor; E-mode: Enhancement mode; D-mode: Depletion mode; 2DEG: Two-dimensional electron gas; MIS: Metal–insulator–semiconductor; FP: Field plate; DFF-HEMT: Double gates flip-structure E-mode HEMT with FP; MIS-FP HEMT: The MIS trench gate HEMT with FP; TG: Top gate; BG: Bottom gate.

Author contributions
Siyu Deng, Jie Wei and Xiaorong Luo designed the concept and analysis. Siyu Deng Cheng Zhang and Dezun Liao conducted the simulation. Siyu Deng, Tao Sun, and Lufan Xi conducted data processing; Siyu Deng and Kemeng Yang wrote the main manuscript. Siyu Deng and Xiaorong Luo modified the paper. All authors read and approved the final manuscript.

Availability of Data and Materials
The data used and analyzed during the current study are available from the corresponding authors upon reasonable request.

Declarations

Ethics Approval and Consent to Participate
All authors of the manuscript have agreed to its content and are accountable for all aspects of the accuracy and integrity of the manuscript.

Consent for Publication
The authors agree to publish. The results/data/figures in this manuscript have not been published elsewhere, nor are they under consideration (from you or one of your Contributing Authors) by another publisher.

Competing interests
The authors declare that they have no competing interests.

References

1. Ishida M, Ueda T, Tanaka T et al (2013) GaN on Si technologies for power switching devices. IEEE Trans Electron Devices 60(3):3053–3059
2. Zhou Q, Chen WJ, Liu SH et al (2013) Schottky-contact technology in InAlN/GaN HEMTs for breakdown voltage improvement. IEEE Trans Electron Devices 60(3):1075–1081
3. Chen KJ, Hberlen O, Lidow A et al (2017) GaN-on-Si power technology: devices and applications. IEEE Trans Electron Devices 64(3):779–795
4. Tao M, Liu S, Xie B et al (2018) Characterization of 880 V normally Off GaN MOSHEMT on silicon substrate fabricated with a plasma-free, self-terminated gate recess process. IEEE Trans Electron Devices. https://doi.org/10.1109/TED.2018.2808345
5. Han PC, Yan ZZ, Wu CH et al (2019) Recess-Free Normally-off GaN MIS-HEMT Fabricated on Ultra-Thin-Barrier AlGaN/GaN Heterostructure. In: 31st International symposium on power semiconductor devices and ICs (ISPSD), Shanghai, China, pp 428–430
6. Yu Z, Zhong Y, Gao H et al (2017) p-GaN gate enhancement-mode HEMT through a high tolerance self-terminated etching process. IEEE J Electron Devices Soc 5(5):340–346
7. Kambayashi H, Satoh Y, Kokawa T et al (2011) High field-effect mobility normally-off AlGaN/GaN hybrid MOS-HFET on Si substrate by selective area growth technique. Solid State Electron 56(1):163–167
8. Zhang Y, Min S, Joglekar SJ et al (2013) High threshold voltage in GaN MOS-HEMTs modulated by fluorine plasma and gate oxide. In: Device research conference, pp 141–142
9. Yang L, Hou B, Mi M et al (2018) High-performance enhancement-mode AlGaN/GaN high electron mobility transistors combined with TiN-based source contact ledge and two-step fluorine treatment. IEEE Electron Device Lett. https://doi.org/10.1109/LED.2018.2864135
10. Xie G, Xu E, Lee J et al (2011) Breakdown voltage enhancement for power AlGaN/GaN HEMTs with air-bridge field plate. IEEE Int Conf Electron Devices Solid-State Circuits 2011:337–340
11. Wu JS, Lee C, Wu CH et al (2021) E-Mode GaN MIS-HEMT using ferroelectric charge trap gate stack with low dynamic on-resistance and high Vth stability by field plate engineering. IEEE Electron Device Lett 42(9):1268–1271
12. Xiong JY, Yang C, Wei J et al (2016) Novel high voltage RESURF AlGaN/GaN HEMT with charged buffer layer. Sci China Inf Sci 59(4):1–10. https://doi.org/10.1007/s11432-015-5454-z
13. Xiao M, Ma Y, Liu K et al (2021) 10 kV, 39 mΩ·cm2 multi-channel AlGaN/GaN Schottky barrier diodes. IEEE Electron Device Lett 42(6):808–811
14. Nakajima A, Sumida Y, Dhyani MH et al (2010) High-density two-dimensional hole gas induced by negative polarization at GaN/AlGaN heterointerface. Applied Phys Express 3(12):1–3
15. Nakajima A, Dhyani MH, Narayanan E et al (2011) GaN based Super HFETs over 700V using the polarization junction concept. In: 2011 IEEE 23rd international symposium on power semiconductor devices and Ics, pp 280–283
16. Chen D, Liu Z, Xing Lu et al (2019) Efficiency improved by monolithic integration of HEMT with vertical-structure LEDs and Mg doping on dry etched GaN. J Mater Chem C 7:2823–2828
17. Yi B, Wu Z et al (2021) Simulation study of a p-GaN HEMT with an integrated Schottky barrier diode. IEEE Trans Electron Devices 68(12):6039–6044
18. Hung TH, Park PS et al (2014) Interface charge engineering for enhancement-mode GaN MISHEMTs. IEEE Electron Device Lett 35(3):312–314. https://doi.org/10.1109/LED.2013.2296659
19. Kajiwara Y, Shindome A et al (2020) Highly Reliable GaN-MOSFETs with High Channel Mobility Gate by Selective-Area Crystallization. In: 32nd international symposium on power semiconductor devices and ICs (ISPSD)

Publisher's Note

Springer Nature remains neutral with regard to jurisdictional claims in published maps and institutional affiliations.